INTERNATIONAL JOURNAL FOR NUMERICAL METHODS IN FLUIDS
Int. J. Numer. Meth. Fluids (2012)
Published online in Wiley Online Library (wileyonlinelibrary.com/journal/nmf). DOI: 10.1002/fld.3694

Development of a compressive surface capturing formulation for modelling free-surface flow by using the volume-of-fluid approach

J. A. Heyns[1,*,†], A. G. Malan[1], T. M. Harms[2] and O. F. Oxtoby[1]

[1]*Advanced Computational Methods Research Group, Aeronautics Systems, Council for Scientific and Industrial Research, Pretoria, South Africa*
[2]*Department of Mechanical Engineering, University of Stellenbosch, South Africa*

SUMMARY

With the aim of accurately modelling free-surface flow of two immiscible fluids, this study presents the development of a new volume-of-fluid free-surface capturing formulation. By building on existing volume-of-fluid approaches, the new formulation combines a blended higher resolution scheme with the addition of an artificial compressive term to the volume-of-fluid equation. This reduces the numerical smearing of the interface associated with explicit higher resolution schemes while limiting the contribution of the artificial compressive term to ensure the integrity of the interface shape is maintained. Furthermore, the computational efficiency of the the higher resolution scheme is improved through the reformulation of the normalised variable approach and the implementation of a new higher resolution blending function. The volume-of-fluid equation is discretised via an unstructured vertex-centred finite volume method and solved via a Jacobian-type dual time-stepping approach. Copyright © 2012 John Wiley & Sons, Ltd.

Received 18 October 2011; Revised 24 April 2012; Accepted 6 May 2012

KEY WORDS: volume-of-fluid; surface capturing; higher resolution schemes; artificial compressive term

1. MODELLING IMMISCIBLE TWO-FLUID FLOW

There are various industries that benefit from the accurate modelling of dynamic two-fluid flow. Examples of these include the casting industry, maritime and naval engineering (where impact loads on fixed and floating structures are studied) as well as in the transportation of fuel and other fluids by means of surface and air. With the numerical modelling of two immiscible fluids or free-surface modelling as it is commonly referred to, it is necessary to accurately describe the evolution of the free-surface interface. Various methods to model this evolution have been proposed in the literature.

One free-surface modelling approach is to model the evolution of the free-surface with Lagrangian surface fitting methods [1–3], where the interface is fitted to the mesh. These methods, however, are limited in the flow phenomena that they can model, as large interface deformations lead to highly distorted meshes that require continuous remeshing. Furthermore, complex procedures are required to model merging and break-up of the interface. With a Eulerian approach, the fluids can either be modelled by means of so-called volume tracking methods or of interface or front tracking techniques. Here, the propagation of the volume or the interface is computed on the basis of the local velocity.

Interface tracking methods include massless particles on the interface [4–6], height functions [7,8] and level set methods [9–11]. Interface or front tracking methods, however, are non-conservative [12–14] and limited in their application to complex flow phenomena such as separation and merging

*Correspondence to: J. A. Heyns, CSIR Advanced Computational Methods, Building 12, Pretoria 0001, South Africa.
†E-mail: jaheyns@gmail.com

of fluids. Extensions to overcome these limitations tend to increase the complexity as well as the computational overhead.

With volume tracking methods, the fluids are represented either with massless particles or with a volume fraction indicator function, where the latter is commonly referred to as the volume-of-fluid (VOF) approach. With these methods, the exact position of the interface is unknown, and special algorithms are required to capture a well-defined interface. With the Marker-and-Cell or the smooth particle hydrodynamics approaches, the fluid of interest is represented by massless particles that are spread over the volume occupied by that fluid [15–17]. Babaei *et al.* [18] note that these methods are computationally expensive and are not well posed in the description of the boundary conditions.

In contrast, VOF volume tracking methods use a volume fraction advection equation to describe the evolution of the fluid volume. These methods are capable of conserving mass [19–21] and have been shown to be effective in modelling separation and merging of fluids. To maintain a sharp interface and ensure the volume fraction remains bounded, a number of approaches have been proposed, namely, discretising the advective term by using non-linear higher resolution schemes and adding an artificial compressive term to the VOF equation.

Another approach is to combine geometric reconstruction of the interface with the VOF method. This helps in maintaining a very sharp interface while ensuring mass conservation. Examples of these schemes are presented in the work of Raessi *et al.* [19], Sun [22] and Cummins *et al.* [21]. Most of these methods focus on two-dimensional structured implementations; however, it must be noted that Aulisa *et al.* [23] and López and Hernández [24] proposed extensions to three dimensions. With the aim of modelling three-dimensional problems evolving complex unstructured meshes, the surface capturing VOF methodology is preferred for this study.

With non-linear higher resolution schemes, the volume fraction face value, α_f, is discretised using either the normalised variable (NV) approach of Leonard [25] with convective boundedness criteria (CBC) or a flux-limiting method employing the total variation diminishing condition. The NV approach is preferred as the availability criteria are easily evaluated [26]. It is however noted that flux-limiting schemes with total variation diminishing are employed by Tsui *et al.* [13] and Cassidy *et al.* [12]. Further advantages of the NV approach are discussed in depth by Wacławczyk and Koronowiczy [27], Ubbink and Issa [28] and Leonard [25], among others.

Although NV higher resolution schemes are highly compressive and capable of maintaining a sharp interface, they are inclined to distort or wrinkle the interface when the free surface is not aligned with the control volume face. As a result, Lafaurie *et al.* [29] developed a scheme that switches between compressive downwinding and diffusive upwinding to maintain a better-defined free-surface interface shape while preventing artificial smearing of the interface. With this concept, various authors developed schemes that switch between compressive and higher resolution schemes, where they are blended on the basis of the alignment of the free-surface interface and the control volume face. These are commonly referred to as blended high-resolution surface capturing schemes, and examples of them include STACS of Darwish and Moukalled [30], CICSAM of Ubbink and Issa [28], HRIC of Muzaferija *et al.* [31] and SURFER of Lafaurie *et al.* [29].

Blended higher resolution schemes tend to be computationally efficient, are easily implemented on unstructured three-dimensional meshes and can be applied in modelling complex flow phenomena such as separation and merging of the interface. However, with these schemes, the degree of numerical smearing is directly proportional to the time-step size, and furthermore, the interface sharpness cannot be recovered once smearing has occurred.

As an alternative to blended higher resolution schemes, Rusche [32] and Jasak and Weller [33] introduced an artificial compressive term into the VOF equation to achieve the necessary compression of the interface. Gopala and van Wachem [20] showed that the inter-gamma scheme of Jasak and Weller [33], with the artificial compressive term, is capable of maintaining a sharp interface but tends to wrinkle the shape of the free-surface interface. Takatani *et al.* [34] introduced an additional anti-diffusion step to sharpen the interface, where the anti-diffusion coefficient is only activated in the interface and is scaled according to the Courant number.

With the aim of accurately modelling the free-surface evolution of two immiscible fluids, a new blended higher resolution artificial compressive (HiRAC) formulation is developed. This formulation reduces the Courant number-related numerical smearing of the interface while maintaining the

DOI: 10.1002/fld

integrity of the interface shape. The new formulation achieves this by building on existing VOF approaches and combining them in a manner as to improve the overall performance and accuracy.

2. VOLUME-OF-FLUID APPROACH

For a two-fluid system, the VOF method involves the construction of an advection equation for the indicator volume fraction, α, to describe the evolution of the free-surface interface

$$\frac{\partial \alpha}{\partial t} + \frac{\partial}{\partial x_i}(\alpha u_i) = 0 \tag{1}$$

where time is denoted t and the velocity and spatial coordinate in direction i are u_i and x_i, respectively.

The volume fraction can be defined as

$$\alpha(x_i, t) = \begin{cases} 1 & \text{for the point } (x_i, t) \text{ inside fluid 1} \\ 0 & \text{for the point } (x_i, t) \text{ inside fluid 2} \end{cases} \tag{2}$$

The VOF equation is discretised using an edge-based vertex-centred (median-dual) finite volume method [35, 36]. A schematic representation of the median-dual-mesh construction on an unstructured grid is shown in Figure 1. To this effect, the VOF equation is spatially discretised in weak form at a node ξ as F1

$$\frac{\partial \alpha}{\partial t} \int_{\mathcal{V}_\xi} \mathrm{d}\mathcal{V}_\xi + \sum_{\Upsilon_\xi \cap \mathcal{V}_\xi} \alpha_f u_f^j C_f^j = 0 \tag{3}$$

where $\mathcal{V}_\xi$ represents the control volume and C_f is the edge coefficient of the edge Υ_ξ, which intersects $\mathcal{V}_\xi$. Further, the f quantities denote the values at the volume face $\mathcal{A}_f$.

2.1. Higher resolution schemes with the normalised variable approach

To ensure an accurate solution when modelling free-surface flow with VOF, a sharp interface between the two fluids needs to be maintained while the volume fraction is kept within its physical bounds of zero and one. To achieve this, the volume fraction face flux, α_f, is interpolated using a blended higher resolution scheme.

As noted earlier, the NV approach with CBC is preferred for the formulation of the blended higher resolution scheme. The normalised variable is found using the expression

$$\tilde{\alpha} = \frac{\alpha - \alpha_U}{\alpha_A - \alpha_U} \tag{4}$$

where the upwind, donor and acceptor cells are denoted U, D and A, respectively.

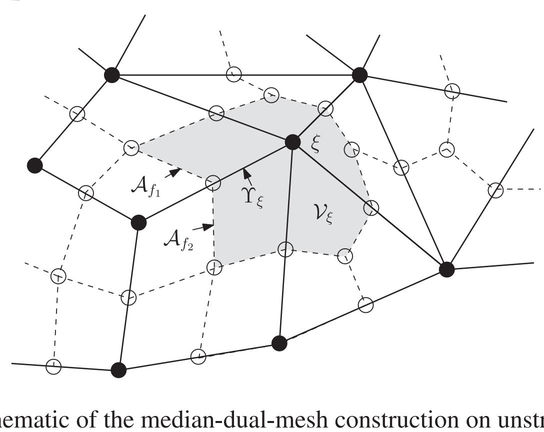

Figure 1. Schematic of the median-dual-mesh construction on unstructured grids.

DOI: 10.1002/fld

To ensure a bounded solution when the NV approach is used to compute the normalised face value, $\tilde{\alpha}_f$, the convective boundedness criteria are typically employed. Leonard [25] adjusted the implicit CBC of Gaskell and Lau [37] for explicit discretisation by introducing a linear weighting based on the cell Courant number, c_f. The explicit formulation of CBC reads

$$\begin{aligned} &\tilde{\alpha}_D \leqslant \tilde{\alpha}_f \leqslant \min\left\{1, \frac{\tilde{\alpha}_D}{c_f}\right\} && \text{for } 0 \leqslant \tilde{\alpha}_D \leqslant 1 \\ &\tilde{\alpha}_f = \tilde{\alpha}_D && \text{for } \tilde{\alpha}_D < 0 \text{ or } \tilde{\alpha}_D > 1 \end{aligned} \tag{5}$$

where the cell Courant number is based on the volumetric fluxes leaving the donor cell and is calculated as described in Ubbink and Issa [28].

For an unstructured formulation of the NV approach, the expression for the projected upwind value (Figure 2) as presented by Ubbink and Issa [28] is used

$$\alpha_U^* = \alpha_A - 2(\nabla\alpha)_D \cdot \mathbf{d} \tag{6}$$

where the edge vector is defined as $\mathbf{d} = \mathbf{x}_A - \mathbf{x}_D$.

2.2. *Artificial compressive term*

To achieve a sharp free-surface interface, Jasak and Weller [33] presented an alternative approach to discretising the volume fraction face flux, α_f, with a blended higher resolution scheme. They introduced an artificial compressive term into the VOF equation to reduce the smearing of the interface. If the said artificial compressive term is added to the VOF Equation (1), the equation reads

$$\frac{\partial\alpha}{\partial t} + \nabla.(u_i\alpha) + \nabla.(u_c|_i\alpha(1-\alpha)) = 0 \tag{7}$$

The term $\alpha(1-\alpha)$ ensures that the artificial compressive term is only activated in the interface region and does not affect the rest of the domain. The compressive velocity, u_c, is proportional to the unit vector normal to the interface, $\mathbf{n}_\alpha$, ensuring optimal compression of the interface

$$u_c = c_\alpha |u_f| \mathbf{n}_\alpha \tag{8}$$

where

$$\mathbf{n}_\alpha = \frac{\nabla\alpha}{|\nabla\alpha|} \tag{9}$$

and c_α is a compressive coefficient and $|u_f|$ is the magnitude of the face velocity.

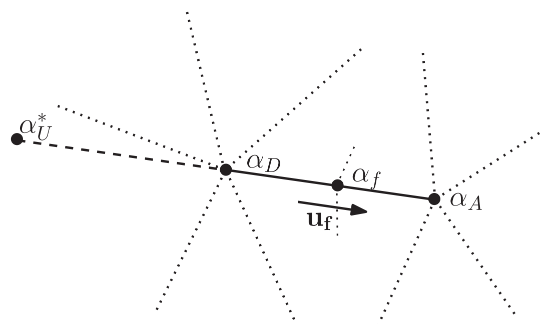

Figure 2. Schematic representation of the normalised variable nomenclature on unstructured meshes.

DOI: 10.1002/fld

3. PROPOSED BLENDED SURFACE CAPTURING FORMULATION

In Section 1, it is argued that each of the VOF approaches presented earlier has its own strengths and weaknesses. Blended higher resolution methods are capable of maintaining the integrity of the interface shape but tend to become diffusive at higher Courant numbers. On the other hand, with the approach of adding an artificial compressive term, it is possible to ensure a sharp free-surface interface at high Courant numbers, but it tends to result in the wrinkling of the interface shape. From the mathematical formulation, it is apparent that these approaches can easily be combined.

A new blended HiRAC scheme is developed. HiRAC aims to reduce the Courant number-related numerical smearing while maintaining a well-defined free-surface interface shape. The method involves discretising the volume fraction face flux by using a blended higher resolution scheme but, in addition, introduces an artificial compressive term to the VOF equation. As the face flux is discretised using a compressive scheme, the degree of additional compression needed from the artificial term is limited, preventing it from distorting the shape of the free-surface interface.

The formulation of the new HiRAC method is divided into three parts: firstly, the appropriate temporal discretisation of the VOF equation is considered on the basis of the availability criteria restrictions; secondly, a computationally efficient blended higher resolution approach for discretising the face flux is presented; and finally, the implementation of the artificial compressive term is considered.

3.1. Temporal discretisation

In Figure 3, the regions for which the convection boundedness criteria ensure a bounded solution are shown. The dark grey area represents the region for an explicit solution, and the lighter grey area represents the extended region for an implicit solution. It is noted that the upper bound of CBC provides the most compressive solution with the sharpest interface, and therefore, as the Courant number increases, the explicit solution tends towards the more diffusive upwind differencing. F3

Because of the explicit schemes' dependence on c_f, Hoekstra *et al.* [38], Hogg *et al.* [39] and Darwish and Moukalled [30] employ implicit formulations to achieve more compressive solutions at larger time steps. By considering non-linear higher resolution discretisation schemes, it is noted

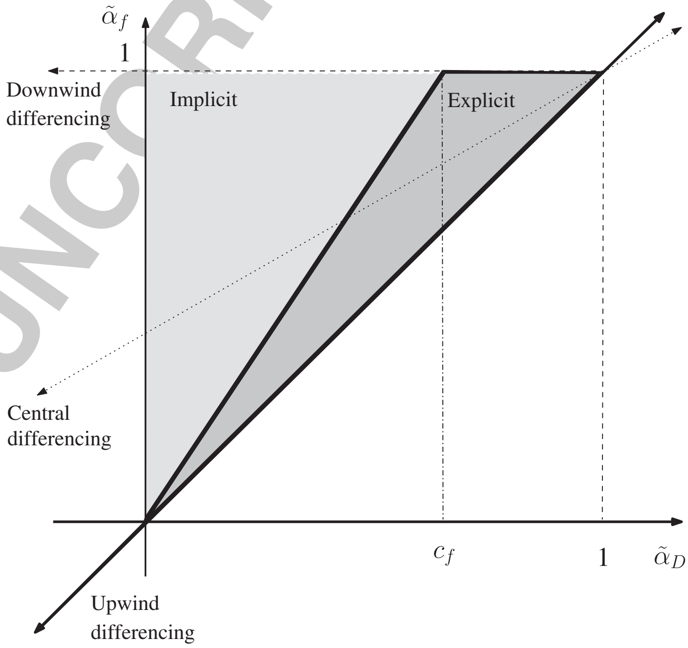

Figure 3. Bounded regions on the normalised variable diagram for explicit and implicit flow calculations.

that they are a function of both the flow direction as well as the local shape or gradient of the volume fraction. As the gradient at the latest time step is unknown, an approximation needs to be made for the implicit formulation. Using Crank–Nicolson for the temporal discretisation, Ubbink and Issa [28] noted that if small time steps are taken, a weighting factor, β_f, can be approximated by using the value at the previous time step. They therefore recommend the use of a Courant number of 0.3. The weighting factor is a function of the local shape and orientation of the volume fraction, is defined as

$$\beta_f = \frac{\tilde{\alpha}_f - \tilde{\alpha}_D}{1 - \tilde{\alpha}_D} \tag{10}$$

and is used to calculate the actual volume fraction face value

$$\alpha_f = (1 - \beta_f)\alpha_D + \beta_f \alpha_A \tag{11}$$

If larger time steps are to be taken, the approximation of β_f would be inaccurate and the solution may become unbounded, as the amount of fluid projected into or out of the cell might exceed the available amount. Therefore, although the implicit schemes are not dependant on the c_f number and tend to be more compressive for larger time steps, it is suggested that for larger time steps, the degree to which the solution will be unbounded also increases. Furthermore, it is noted that the interface is localised to relatively small regions of the domain, and it would most likely be computationally inefficient to use costly implicit solvers.

It appears that explicit schemes tend to become diffusive for larger time steps and the approximated implicit schemes result in a costly, unbounded solution. For the purpose of this work, it is proposed that a Jacobi-type solver with dual time-stepping be employed, where the volume fraction equation is solved in pseudotime, t_τ. This approach results in the advection of the volume fraction being broken up into pseudo substeps, providing an efficient way of implementing the substepping philosophy suggested by Gopala and van Wachem [20].

As proposed by Ubbink [26], HiRAC employs a second-order Crank–Nicholson formulation but introduces a Jacobi-type dual time-stepping approach. The semi-discrete VOF equation with the addition of an artificial compressive term reads

$$\frac{\alpha^{\tau+1} - \alpha^{\tau}}{\Delta t_\tau} + \frac{\alpha^{\tau} - \alpha^{n}}{\Delta t} = -\frac{1}{2}\left[\left.\frac{\partial (u_i \alpha)}{\partial x_i}\right|^{\tau} + \left.\frac{\partial (u_i \alpha)}{\partial x_i}\right|^{n}\right] - \frac{\partial}{\partial x_i}[u_c|_i \alpha(1-\alpha)]|^{\tau} \tag{12}$$

where the implicit solution is approached as it converges in pseudotime. The pseudo-time step is calculated as suggested in the work of Malan *et al.* [40]. As the volume fraction is evaluated at every pseudo-time step and the availability criteria satisfied, no approximation of a weighting factor needs to be made and the restriction on the Cournant number disappears. The dual time-stepping formulation, therefore, is better enabled to provide a bounded and compressive solution at higher c_f numbers.

3.2. *Fast higher resolution formulation*

As mentioned earlier, the volume fraction face value is interpolated using the NV approach with CBC to ensure a monotonic solution. Whereas, for the interpolation of the velocity face value in the advective term, it is found that by employing a linear third-order upwinding scheme, acceptable results are obtained. The focus, therefore, falls on the formulation of a suitable interpolation scheme for the volume fraction face value.

Q2 Numerous studies have compared various blended higher resolution schemes, where ~~CICSAM~~ and ~~HRIC~~ are most commonly used as reference in the comparative analyses. Hoekstra *et al.* [38] show that CICSAM performs better than HRIC, but note that both schemes are highly dependent on the Courant number, c_f, as well as grid refinement. Similar conclusions are made by Tsui *et al.* [13], Wacławczyk and Koronowiczy [27] and Gopala and van Wachem [20]. They found that CICSAM preserves the shape of the interface more accurately, maintaining a sharper interface. They note that the interface smears as the c_f number increases.

DOI: 10.1002/fld

Ubbink and Issa [28] suggest the use of the compressive Hyper-C differencing scheme, which follows the upper bound of the CBC, helping to maintain a sharp free-surface interface. HRIC utilises a bounded downwind scheme, which is similar to Hyper-C [30]. The Hyper-C formulation of Leonard [25] expressed in terms of the normalised variables of Equation (4) is

$$\tilde{\alpha}_{f_{HC}} = \begin{cases} \min\left\{1, \frac{\tilde{\alpha}_D}{c_f}\right\} & \text{for } 0 \leqslant \tilde{\alpha}_D \leqslant 1 \\ \tilde{\alpha}_D & \text{for } \tilde{\alpha}_D < 0 \text{ or } \tilde{\alpha}_D > 1 \end{cases} \tag{13}$$

As the system is solved in pseudotime, the discretised face values used in the dual time-stepping formulation at time step τ and n can be calculated directly. This makes it possible with HiRAC to reformulate the normalised variable Hyper-C scheme to be computationally efficient. As it is no longer necessary to transform the volume fractions to and from normalised variables, the number of calculations are subsequently reduced. For HiRAC, the normalised variables in Equation (13) are accordingly written in terms of the actual volume fractions:

$$\alpha_{f_{HC}} = \begin{cases} \min\left\{\alpha_A, \frac{\alpha_D - \alpha_U^*}{c_f} + \alpha_U^*\right\} & \text{for } r^* > 1 \text{ and } \alpha_D > \alpha_U^* \\ \max\left\{\alpha_A, \frac{\alpha_D - \alpha_U^*}{c_f} + \alpha_U^*\right\} & \text{for } r^* > 1 \text{ and } \alpha_D < \alpha_U^* \\ \alpha_D & \text{for } r^* \leqslant 1 \end{cases} \tag{14}$$

where the gradient, r^*, is defined as

$$r^* = \frac{\alpha_A - \alpha_U^*}{\alpha_D - \alpha_U^*} \tag{15}$$

To preserve the shape of the free-surface interface, the CICSAM scheme blends the compressive Hyper-C scheme with the high resolution ULTIMATE-QUICKEST scheme of Leonard [25]. On the other hand, HRIC and ~~STACS~~ use respectively Upwind and STOIC. On the basis of the findings of Tsui *et al.* [13] and Wacławczyk and Koronowiczy [41], when comparing blended higher resolution schemes, HiRAC also employs ULTIMATE-QUICKEST, which reads

$$\tilde{\alpha}_{f_{UQ}} = \begin{cases} \min\left\{\frac{8c_f\tilde{\alpha}_D + (1-c_f)(6\tilde{\alpha}_D + 3)}{8}, \tilde{\alpha}_{f_{HC}}\right\} & \text{for } 0 \leqslant \tilde{\alpha}_D \leqslant 1 \\ \tilde{\alpha}_D & \text{for } \tilde{\alpha}_D < 0 \text{ or } \tilde{\alpha}_D > 1 \end{cases} \tag{16}$$

In a similar manner as was performed for Hyper-C, the computational efficiency of ULTIMATE-QUICKEST can be improved by expanding the normalised variables. For HiRAC, Equation (16) can be written in terms of the actual volume fractions

$$\alpha_{f_{UQ}} = \begin{cases} \min\left\{k^*, \alpha_{f_{HC}}\right\} & \text{for } r^* > 1 \text{ and } \alpha_D > \alpha_U \\ \max\left\{k^*, \alpha_{f_{HC}}\right\} & \text{for } r^* > 1 \text{ and } \alpha_D < \alpha_U \\ \alpha_D & \text{for } r^* \leqslant 1 \end{cases} \tag{17}$$

where r^* is the same as in Equation (15) and

$$k^* = \alpha_U + \left[\frac{3 + c_f}{4}\right](\alpha_D - \alpha_U) + \frac{3(1 - c_f)}{8}(\alpha_A - \alpha_U) \tag{18}$$

For the blended schemes, a weighting factor, γ, is used to switch between the compressive and more diffusive schemes on the basis of the alignment of the free-surface interface and the control volume face, yielding a blended face value

$$\cancel{\tilde{\alpha} = \gamma_f \tilde{\alpha}_{f_{HC}} + (1 - \gamma_f)\tilde{\alpha}_{f_{UQ}}} \tag{19}$$

DOI: 10.1002/fld

The weighting function suggested by Ubbink and Issa [28] to blend the compressive and diffusive schemes is

$$\gamma_f = \min\left\{k_\gamma \frac{\cos(2\theta_f)+1}{2}, 1\right\} \tag{20}$$

where they recommend $k_\gamma = 1$ and

$$\theta_f = \arccos\left|\frac{(\nabla\alpha)_D \cdot \mathbf{d}}{|(\nabla\alpha)_D| \cdot |\mathbf{d}|}\right| \tag{21}$$

Tsui *et al.* [13] and Darwish and Moukalled [30] use the switching formulation

$$\gamma_f = \cos^4(\theta_f) \tag{22}$$

Both of the formulations given make use of computationally expensive cos and arccos computations. To improve the efficiency of the scheme, it is suggested that the weighting function is defined as

$$\gamma_f = \min\left((\eta_f)^m, 1\right) \tag{23}$$

where

$$\eta_f = \left|\frac{(\nabla\alpha)_D \cdot \mathbf{d}}{|(\nabla\alpha)_D| \cdot |\mathbf{d}|}\right| \tag{24}$$

F4 In Figure 4, the new weighting factor is plotted as a function of η_f, alongside existing weighting factors. For $m = 2$, the new formulation reduces to the weighting function of Ubbink and Issa [28], for $k_\gamma = 1$, and for $m = 4$, it reduces to the scheme of Tsui *et al.* [13] and Darwish and Moukalled [30]. As m is increased, the interpolation becomes more biased towards the diffusive higher resolution scheme. For this study, $m = 2$ is used as it provides a good balance between the compressive and diffusive higher resolution schemes.

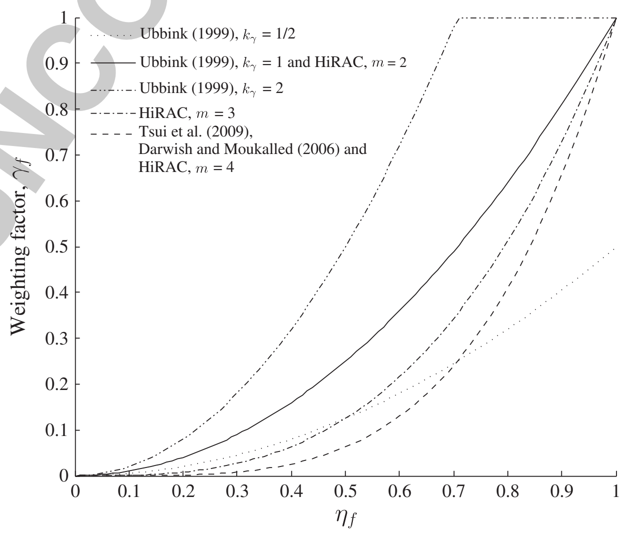

Figure 4. Comparison of the different weighting functions.

DOI: 10.1002/fld

3.3. *Artificial compressive term*

To reduce the inherent numerical diffusivity associated with the higher resolution schemes, we introduce an additional artificial compressive term to the VOF equation. The semi-discrete VOF equation with the artificial compressive term now follows at the dual volume $\mathcal{V}_\xi$:

$$\frac{\partial \alpha}{\partial t}\int_{\mathcal{V}_\xi} \mathrm{d}\mathcal{V} + \sum_{\Upsilon_\xi \cap \mathcal{V}_\xi} \alpha_f u_f^j C_f^j + \sum_{\Upsilon_\xi \cap \mathcal{V}_\xi} \alpha_f (1-\alpha_f)\, u_{c\,f}^j C_f^j = 0 \qquad (25)$$

By considering the discretised artificial compressive term, the interpolation of the volume fraction face value, α_f, is already discussed in the previous section and only the compressive velocity needs to be determined. The compressive velocity is calculated using the expression

$$u_{c\,f} = c_\alpha |u_f| \mathbf{n}_\alpha \qquad (26)$$

where u_f is the discretised velocity face value and, as noted previously, is calculated using third-order upwinding.

The compressive coefficient, c_α, is selected according to the temporal and spatial discretisation methodology used. Rusche [32], using the inter-gamma scheme of Jasak and Weller [33], states that $c_\alpha = 1.5$ is desirable. For HiRAC with the compressive blended higher resolution scheme and dual time-stepping, it is found that the best results are obtained for all test cases (Section 4) with a compressive coefficient value of $c_\alpha = 0.1$. The required contribution from the artificial compressive term with HiRAC is therefore notably less than for the inter-gamma scheme.

As the volume fraction undergoes a large change in gradient over the free-surface interface, it is found that the vector normal to the interface is calculated inaccurately if Equation (9) is discretised directly. To remedy this, a smoothed volume fraction value, α^*, is used to calculate $\mathbf{n}_\alpha$

$$\mathbf{n}_\alpha^* = \frac{\nabla \alpha^*}{|\nabla \alpha^*|} \qquad (27)$$

Various methods can be used to smooth the volume fraction, where the convolution of α with a smooth integration kernel is most commonly implemented [21, 42, 43]. Ubbink and Issa [28] note that, for an edge-based approach, only the information of the two nodes connected to the edge is known and it may become costly to extend the method beyond the direct neighbouring nodes of each cell. This is particularly the case on three-dimensional unstructured meshes. Ubbink and Issa [28] therefore employed a Laplacian filter, $\mathcal{F}$, recommended by Lafaurie *et al.* [29], and adapted it for unstructured meshes

$$\mathcal{F}(\alpha) = \sum_{f=1}^{n} \alpha_f |\mathbf{A}_f| \Bigg/ \sum_{f=1}^{n} |\mathbf{A}_f| \qquad (28)$$

where α_f is determined using central differencing and A_f is the outward pointing area vector. The filter is repeated m times yielding a smooth function, where it is typical to use $m = 2$.

Rusche [32], on the other hand, smoothed the volume fraction by means of elliptic relaxation

$$\left[\nabla.\left(\left(\frac{c}{|\mathbf{d}|}\right)^2 \nabla \alpha^*\right)\right] = \alpha^* + \alpha \qquad (29)$$

where $\mathbf{d}$ is the edge vector and the smoothed volume fraction, α^*, is solved using a costly, implicit solver.

In the interest of efficiency, HiRAC employs a pseudo-explicit diffusive equation to smooth α. With this formulation, the volume fraction is smoothed by evolving the equation in pseudotime

$$\frac{\alpha^{*\,\tau+1} - \alpha^{*\,\tau}}{\Delta \tau} + \nabla \cdot \nabla \alpha^{*\,\tau} = 0 \qquad (30)$$

where typically two iterations are needed.

DOI: 10.1002/fld

In this section, the formulation and implementation of a new VOF surface capturing scheme are presented. The temporal and spacial discretisation of the VOF equation is considered along with the implementation of combining the artificial compressive term with a blended higher resolution scheme. For added computational efficiency, the normalised variable approach used in the development of the higher resolution scheme is reformulated and a new higher resolution blending function is proposed.

4. COMPARATIVE ANALYSIS

To assess the increase in accuracy as well as improved efficiency of the developed HiRAC formulation, a comparative analysis is performed with CICSAM as benchmark. The latter provides a good point of reference as is typically used in benchmarking schemes [13, 20, 27], and furthermore, HiRAC builds on CICSAM. However, as higher c_f numbers need to be evaluated, CICSAM is temporally discretised using the dual time-stepping formulation of HiRAC.

To evaluate the reduction in computational cost of the reformulated higher resolution interpolation of the volume fraction face value, the advection of a one-dimensional step function is considered. To measure the possible gain in CPU time, the normalised gradient of Equation (24) is assumed to be $\eta_f = 0.5$ so that the combined computational cost of the reformulated Hyper-C and ULTIMATE-QUICKEST schemes as well as the new weighting function is measured. In Figure 5, the CPU cost as a function of mesh size is shown. It is noted that, in the figure, the reformulated higher resolution interpolation used for HiRAC may realise a computational gain of approximately 60% when solving the VOF equation. The reduction in overall solver solution time, however, would be highly dependent on which type of flow solver is coupled to the VOF equation. It is found that the contribution to the reduction in CPU time due to the reformulation of the normalised variable approach and the new weighting factor is more or less equal.

To evaluate HiRAC, various benchmarked test cases are considered, where the surface capturing scheme is subject to different possible flow phenomena with complex interface motion. The numerical solution is compared quantitatively by means of error estimates as well as by visual comparison of contour plots. As part of the comparative analyses, both structured as well as unstructured meshes are used. The test cases considered are the following:

- advection of round and square droplets;
- rotating key;
- droplet in shear flow;
- falling droplet; and
- three-dimensional sphere undergoing rotation and translation.

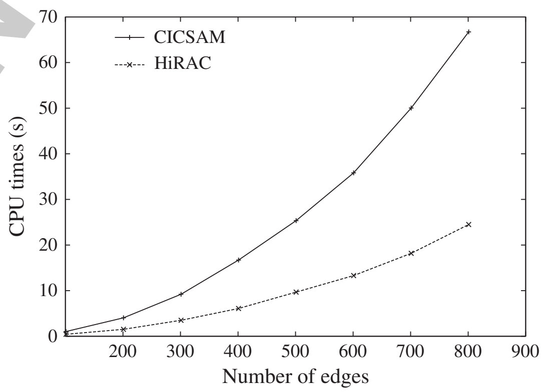

Figure 5. CPU time for one-dimensional advection of a step function by using blended higher resolution schemes.

DOI: 10.1002/fld

The criterion most commonly used to evaluate surface capturing schemes is a comparative error analysis [12, 20, 28]. For the comparative analysis, the numerical result is compared with the expected analytical solution to sense the average error computed as

$$E_{\text{comp}} = \frac{1}{N} \sum_{i=1}^{N} |\alpha_{\text{analt}} - \alpha_i| \tag{31}$$

which provides an indication of the degree of interface deformation and smearing.

For test cases where the analytical solution is unknown, it is proposed that a diffusive error formulation be used to evaluate the associated numerical smearing of the interface

$$E_{\text{diff}} = \frac{4}{N} \sum_{i=1}^{N} |\alpha_i||1 - \alpha_i| \tag{32}$$

where E_{diff} is equal to zero if there are no partially filled cells. As smearing of the interface causes the inaccurate distribution of partially filled cells over the computational domain, the diffusive error E_{diff} provides a way of quantifying the diffusivity of the surface capturing scheme.

4.1. Advected square and round droplets

Comparing surface capturing schemes, various authors [20, 26, 38] considered the convection of different forms of droplets through space. In this study, the advection of a 0.3×0.3 square droplet (Figure 6) and a 0.3-diameter round droplet is considered. The droplets are advected at a rate of F6 $(0.015, 0.0075)$ units/s, where the initial centre point is at (0.2, 0.2) and the final centre point is at (0.8, 0.5).

In Figure 7a, the results for the square droplet using three different structured meshes (80×80, F7 100×100 and 120×120) are shown, and in Figure 7b, the results for the round droplet using a structured 100×100 mesh. It is noted that the error reduces as the meshes are refined and that the relative proportional gain remains more or less the same for the different mesh sizes. In the figures, it is seen that HiRAC provides a notable improvement as Courant number increases.

Contour plots from the numerical solution of the square and round droplets are respectively shown in Figures 8 and 9 for a Courant number of 0.6. For all the analyses, the contour lines are evenly F8 F9 spaced between 0 and 1 with interval of 0.2. The solution for CICSAM is shown on the left and for HiRAC on the right. From the contour plots, it is found that HiRAC maintains a sharper interface for larger c_f numbers, without distorting the interface.

4.2. Rotating key

The rotating key test case is used by various authors including Gopala and van Wachem [20], Wacławczyk and Koronowiczy [41], Darwish and Moukalled [30], Ubbink [26] and Zalesak [44] to

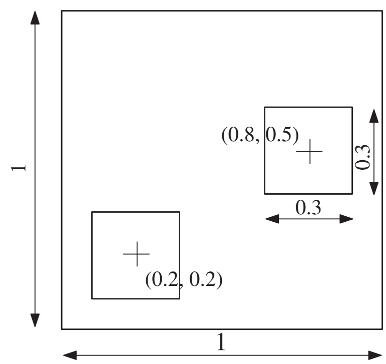

Figure 6. Schematic representation of the advected square and round droplets.

DOI: 10.1002/fld

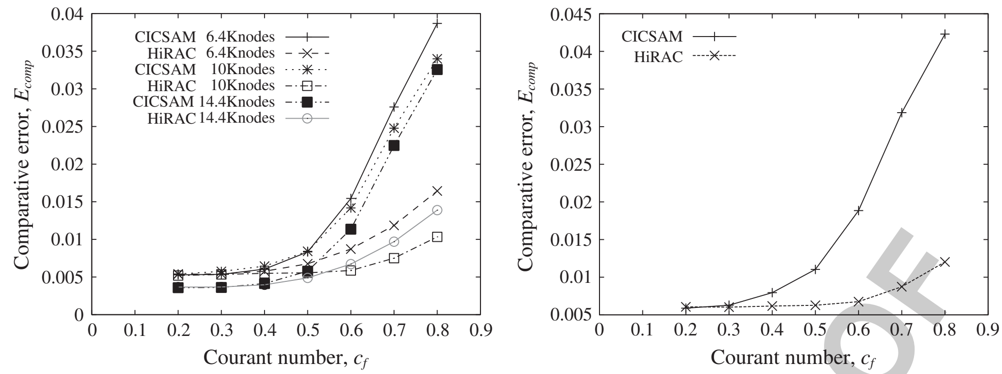

(a) Advecting square droplet (b) Advecting round droplet

Figure 7. Comparative error as a function of the Courant number.

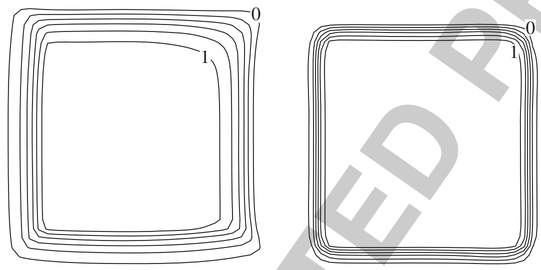

(a) CICSAM (b) HiRAC

Figure 8. Contour plots of the convected square droplet, $c_f = 0.6$.

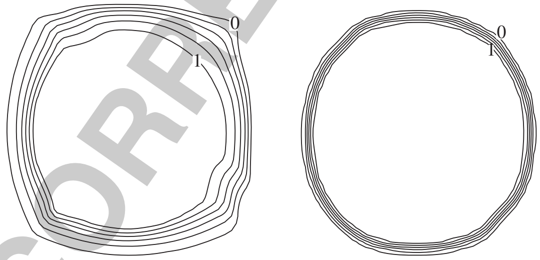

(a) CICSAM (b) HiRAC

Figure 9. Contour plots of the convected round droplet, $c_f = 0.6$.

evaluate different surface capturing schemes. In Figure 10, dimensions of the rotating key, a slotted circle that is rotated around its centre, are shown. A unidirectional velocity field is applied where $u = -\pi/2(y - y_0)$ and $v = \pi/2(x - x_0)$, and the rotating key centre is $(x_0, y_0) = (0.5, 0.5)$. For this analysis, a structured mesh is used to represent the 1×1 computational domain. F10

After one rotation, the numerical results are evaluated and compared with the analytical solution. F11 In Figure 11, the comparative error is plotted as a function of the Courant number. As with the previous test case, it is shown that HiRAC is to a considerably smaller degree dependent on the Courant number.

Contour plots of the solution after one rotation for both CICSAM and HiRAC are shown in F12 Figure 12. Here again, it is found that HiRAC ensures a sharper interface while maintaining an accurate representation of the interface shape.

DOI: 10.1002/fld

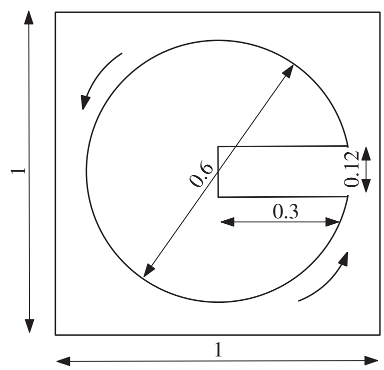

(a) RotatingKey

Figure 10. Schematic representation of the rotating key.

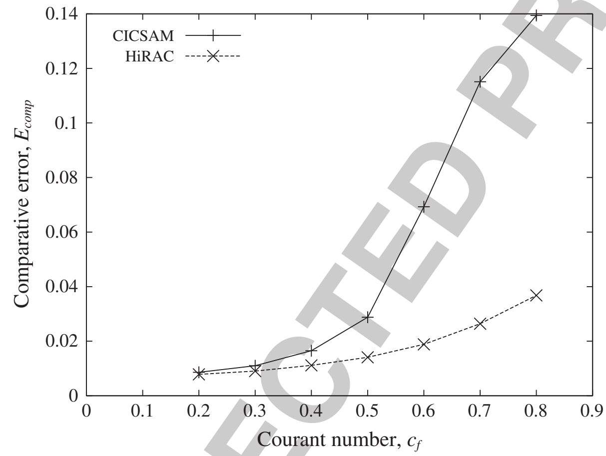

Figure 11. Comparative error as a function of the Courant number for the rotating key.

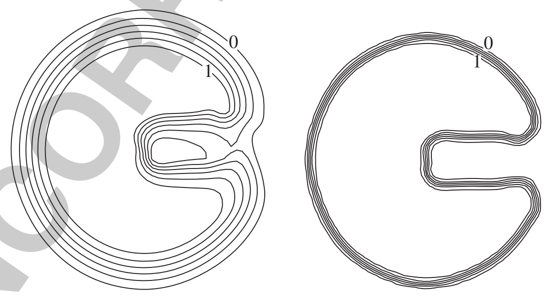

(a) CICSAM (b) HiRAC

Figure 12. Contour plots of the rotating key, $c_f = 0.6$.

4.3. Round droplet in shear flow

Gopala and van Wachem [20], Wacławczyk and Koronowiczy [41] and Hogg *et al.* [39] evaluated the integrity of surface capturing schemes by considering a round droplet placed in a shear flow field. With this test case, the ability of the scheme to handle shearing and stretching of the interface is evaluated. A droplet is placed off centre in a rotating flow field as shown in Figure 13. The pre- **F13**
scribed velocity field is $u = \sin(\pi(x-x_0))\cos(\pi(y-y_0))$ and $v = -\cos(\pi(x-x_0))\sin(\pi(y-y_0))$, where the domain centre is $(x_0, y_0) = (0.5, 0.5)$. After one rotation, the flow field is reversed with the aim of recovering the original round droplet. For this analysis, an unstructured triangular mesh with 5000 nodes is used to represent the ~~computation~~. **Q3**

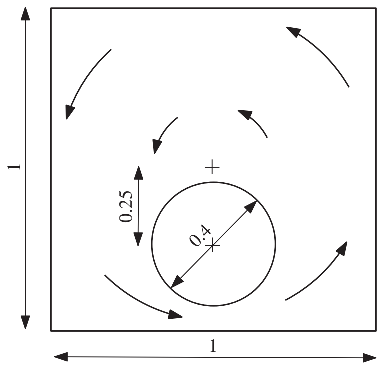

Figure 13. Schematic representation of the droplet in shear flow.

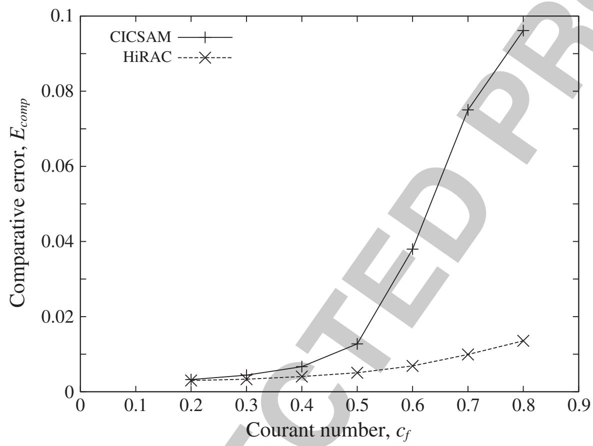

Figure 14. Comparative error as a function of the Courant number for the droplet in shear flow.

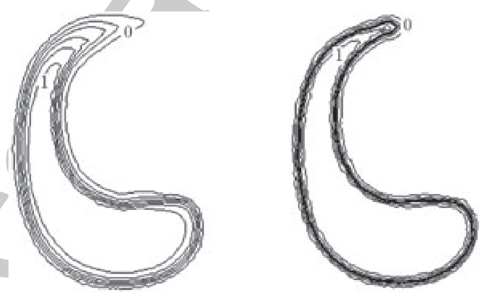

(a) CICSAM (b) HiRAC

Figure 15. Contour plots of the droplet in shear flow just before the flow field is reversed, $c_f = 0.5$.

The schemes are evaluated on the basis of their capability to reproduce the original droplet. In Figure 14, the comparative error is plotted as a function of the Courant number. For the droplet in shear flow on an unstructured mesh, it is also found that comparative error for HiRAC is only to a relatively small degree dependant on the Courant number.

Contour plots of the droplet in shear flow are shown in Figures 15 and 16. In Figure 15, the droplet is shown after it has completed one rotation and just before the flow field is reversed, and in Figure 16, the recovered droplet is shown. Both HiRAC contour plots show that a sharper interface is achieved without distorting the shape of the interface, reproducing the original droplet more accurately.

DOI: 10.1002/fld

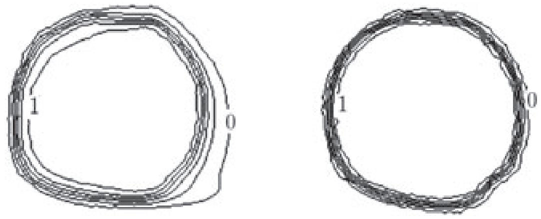

(a) CICSAM (b) HiRAC

Figure 16. Contour plots of the droplet in shear flow after initial shape is recovered, $c_f = 0.5$.

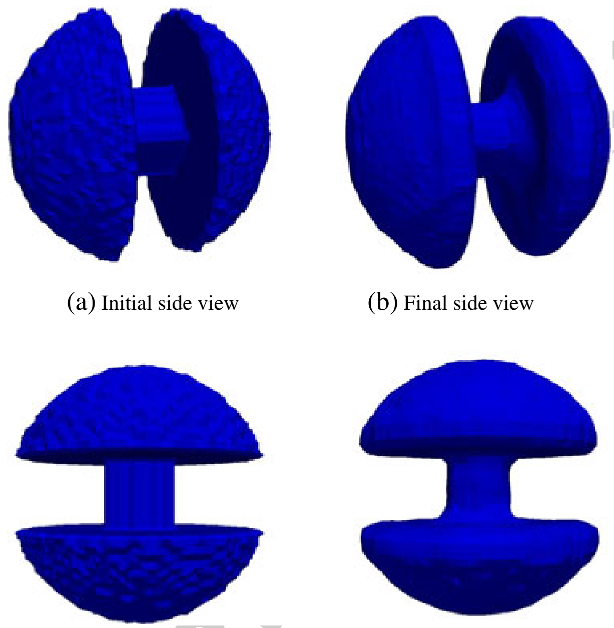

(a) Initial side view (b) Final side view

(c) Initial top view (d) Final top view

Figure 17. Contour plots, $\alpha = 0.5$, of the slotted sphere before and after translation and rotation.

Color Online, B&W in Print

4.4. Evaluation of HiRAC for three-dimensional unstructured meshes

To demonstrate the extension to three-dimensional unstructured meshes, a slotted sphere that is convected and rotated in space is shown. The slotted sphere is convected in the $x - y$ plane and rotated around its x-axis. In Figure 17, the initial contour plot ($\alpha = 0.5$) is shown on the left, and the contour plot of the slotted sphere after it is convected through the domain and has done one rotation around the x-axis is shown on the right. When comparing the contour plots in Figure 17, it is noted that the shape of the interface is quite well preserved. F17

5. CONCLUSION

In conclusion, a new fast VOF compressive surface capturing formulation for modelling immiscible two-fluid flow is developed. HiRAC combines a computationally efficient blended high resolution scheme, which ensures the shape of the interface is preserved, with an artificial compressive term that increases the sharpness of the interface. It is shown that the new HiRAC formulation provides a significant improvement in accuracy at higher Courant numbers by reducing numerical diffusivity and ensuring a sharper interface. Furthermore, the scheme proves to be capable of modelling complex interface phenomena on unstructured three-dimensional meshes.

DOI: 10.1002/fld

REFERENCES

1. de Sousa FS, Mangiavacchi N, Nonato LG, Castelo A, Tom MF, Ferreira VG, Cuminato JA, McKee S. A front-tracking/front-capturing method for the simulation of 3D multi-fluid flows with free surfaces. *Journal of Computational Physics* 2004; **198**(2):469–499.
2. Ferziger JH, Peric M. *Computational Methods for Fluid Dynamics*. Springer-Verlag: New York, 1999.
3. Clarke A, Issa RI. A numerical model of slug flow in vertical tubes. *Computers and Fluids* 1997; **26**(4):395–415.
4. Terashima H, Tryggvason G. A front-tracking method with projected interface conditions for compressible multi-fluid flows. *Computers & Fluids* 2010; **39**(10):1804–1814.
5. Popinet S, Zaleski S. A front-tracking algorithm for accurate representation of surface tension. *International Journal for Numerical Methods in Fluids* 1999; **30**(6):775–793.
6. Unverdi SO, Tryggvason G. A front-tracking method for viscous, incompressible, multi-fluid flows. *Journal of Computational Physics* 1992; **99**(1):180–180.
7. López J, Hernández J. On reducing interface curvature computation errors in the height function technique. *Journal of Computational Physics* 2010; **229**(13):4855–4868.
8. Farmer J, Martinelli L, Jameson A. Fast multigrid method for solving incompressible hydrodynamic problems with free surfaces. *AIAA Journal* 1994; **32**(6):1175–1182.
9. Chen Y, Price W, Temarel P. Numerical simulation of liquid sloshing in LNG tanks using a compressible two-fluid flow model. *Proceedings of the 19th International Offshore and Polar Engineering Conference*, 2009.
10. Sethian J. Level set methods and fast marching methods. *Journal of Computing and Information Technology* 2003; **11**(1):1–2.
11. Sussman M, Almgren AS, Bell JB, Colella P, Howell LH, Welcome ML. An adaptive level set approach for incompressible two-phase flows. *Journal of Computational Physics* 1999; **148**(1):81–124.
12. Cassidy DA, Edwards JR, Tian M. An investigation of interface-sharpening schemes for multi-phase mixture flows. *Journal of Computational Physics* 2009; **228**(16):5628–5649.
13. Tsui YY, Lin SW, Cheng TT, Wu TC. Flux-blending schemes for interface capture in two-fluid flows. *International Journal of Heat and Mass Transfer* 2009; **52**(23-24):5547–5556.
14. Bonometti T, Magnaudet J. An interface-capturing method for incompressible two-phase flows. Validation and application to bubble dynamics. *International Journal of Multiphase Flow* 2007; **33**(2):109–133.
15. Reddy DN, Radosavljevic D. Verification of numerical methods applied to sloshing studies in membrane tanks of lng ships. *International Conference - ICSOT 2006: Design, Construction and Operation of Natural Gas Carriers and Offshore Systems*, 2006; 163–178.
16. Armenio V, Rocca ML. On the analysis of sloshing of water in rectangular containers: Numerical study and experimental validation. *Ocean Engineering* 1996; **23**(8):705–739.
17. Hwang WS, Stoehr RA. Molten metal flow pattern prediction for complete solidification analysis of near net shape castings. *Materials Science and Technology* 1988; **4**(3):240–250.
18. Babaei R, Abdollahi J, Homayonifar P, Varahram N, Davami P. Improved advection algorithm of computational modeling of free surface flow using structured grids. *Computer Methods in Applied Mechanics and Engineering* 2006; **195**(7-8):775–795.
19. Raessi M, Mostaghimi J, Bussmann M. A volume-of-fluid interfacial flow solver with advected normals. *Computers & Fluids* 2010; **39**(8):1401–1410.
20. Gopala VR, van Wachem BG. Volume of fluid methods for immiscible-fluid and free-surface flows. *Chemical Engineering Journal* 2008; **141**(1-3):204–221.
21. Cummins SJ, Francois MM, Kothe DB. Estimating curvature from volume fractions. *Computers & Structures* 2005; **83**(6-7):425–434.
22. Sun M. Volume-tracking of subgrid particles. *International Journal for Numerical Methods in Fluids* 2011; **66**(12):1530–1554.
23. Aulisa E, Manservisi S, Scardovelli R, Zaleski S. Interface reconstruction with least-squares fit and split advection in three-dimensional cartesian geometry. *Journal of Computational Physics* 2007; **225**(2):2301–2319.
24. López J, Hernández J. Analytical and geometrical tools for 3d volume of fluid methods in general grids. *Journal of Computational Physics* 2008; **227**(12):5939–5948.
25. Leonard BP. The ultimate conservative difference scheme applied to unsteady one-dimensional advection. *Computer Methods in Applied Mechanics and Engineering* 1991; **88**(1):17–74.
26. Ubbink O. Numerical prediction of two fluid systems with sharp interfaces. *Ph.D. Thesis*, Department of Mechanical Engineering, Imperial College, London, 1997.
27. Wacławczyk T, Koronowiczy T. Comparison of cicsam and HRiC high-resolution schemes for interface capturing. *Journal of Theoretical and Applied Mechanics* 2008; **46**(2):325–345.
28. Ubbink O, Issa RI. A method for capturing sharp fluid interfaces on arbitrary meshes. *Journal of Computational Physics* 1999; **153**:26–50.
29. Lafaurie B, Nardone C, Scardovelli R, Zaleski S, Zanetti G. Modelling merging and fragmentation in multiphase flows with surfer. *Journal of Computational Physics* 1994; **113**(1):134–147.
30. Darwish M, Moukalled F. Convective schemes for capturing interfaces of free-surface flows on unstructured grids. *Numerical Heat Transfer, Part B: Fundamentals* 2006; **49**(1):19–42.
31. Muzaferija S, Peric M, Sames P, Schellin T. A two-fluid navier-stokes solver to simulate water entry. *Proc 22nd Symposium on Naval Hydrodynamics*, 1998; 277–289.

Q4

Q5

DOI: 10.1002/fld

32. Rusche H. Computational fluid dynamics of dispersed two-phase flows at high phase fractions. *Ph.D. Thesis*, Imperial College, University of London, 2002.
33. Jasak H, Weller HG. Interface tracking capabilities of the inter-gamma differencing scheme. *Technical Report*, Technical report, CFD research group, Imperial College, London, 1995, 1995. Q6
34. Takatani K. Mathematical modeling of incompressible ~~mhd~~ flows with free surface. *ISIJ International* 2007; **47**(4):545–551. Q7
35. Malan AG, Meyer JP, Lewis RW. Modelling non-linear heat conduction via a fast matrix-free implicit unstructured-hybrid algorithm. *Computer Methods in Applied Mechanics and Engineering* 2007; **196**(45-48):4495–4504.
36. Visser C, Malan AG, Meyer JP. An artificial compressibility algorithm for modelling natural convection in saturated packed pebble beds: a heterogeneous approach. *International Journal for Numerical Methods in Engineering* 2008; **75**:1214–1237.
37. Gaskell P, Lau A, Wright N. Comparison of two solution strategies for use with higher-order discretization schemes in fluid flow simulation. *International Journal for Numerical Methods in Fluids* 1988; **8**(10):1203–1215.
38. Hoekstra M, Vaz G, Abiel B, Bunnik T. Free-surface flow modelling with interface capturing techniques. *International Conference on Computational Methods in Marine Engineering*, 2007. Q8
39. Hogg P, Gu X, Emerson D. An implicit algorithm for capturing sharp fluid interfaces in the volume of fluid advection method. *Proceedings of European Conference on Computational Fluid Dynamics-ECCOMAS CFD*, 2006.
40. Malan AG, Lewis RW, Nithiarasu P. An improved unsteady, unstructured, artificial compressibility, finite volume scheme for viscous incompressible flows: Part I. Theory and implementation. *International Journal for Numerical Methods in Engineering* 2002; **54**(5):695–714.
41. Wacławczyk T, Koronowiczy T. Modeling of the wave breaking with CICSAM and HRIC high-resolution schemes. In *European Conference on Computational Fluid Dynamics ECCOMAS CFD*, Wesseling S, Oñate E, Périaux J (eds), 2006. Q9
42. Williams M, Kothe D, Puckett E. Convergence and accuracy of kernel-based continuum surface tension models. *Technical Report*, Los Alamos National Lab., NM (US), 1998.
43. Brackbill J, Kothe D, Zemach C. A continuum method for modeling surface tension. *Journal of Computational Physics* 1992; **100**(2):335–354.
44. Zalesak S. Fully multidimensional flux-corrected transport algorithms for fluids. *Journal of Computational Physics* 1979; **31**(3):335–362.

DOI: 10.1002/fld

Author Query Form

Journal: International Journal for Numerical Methods in Fluids

Article: fld_3694

Dear Author,

During the copyediting of your paper, the following queries arose. Please respond to these by annotating your proofs with the necessary changes/additions.

- If you intend to annotate your proof electronically, please refer to the E-annotation guidelines.
- If you intend to annotate your proof by means of hard-copy mark-up, please refer to the proof mark-up symbols guidelines. If manually writing corrections on your proof and returning it by fax, do not write too close to the edge of the paper. Please remember that illegible mark-ups may delay publication.

Whether you opt for hard-copy or electronic annotation of your proofs, we recommend that you provide additional clarification of answers to queries by entering your answers on the query sheet, in addition to the text mark-up.

Query No.	Query	Remark
Q1	AUTHOR: The citation Figure 3 has been changed to Figure 2. Please check if appropriate; if not, please indicate where Figure 2 should be cited in the text.	In order
Q2	AUTHOR: Please define CICSAM and HRIC.	See recommendation
Q3	AUTHOR: "Computational" has been changed to "computation". Please check if appropriate.	See recommendation
Q4	AUTHOR: Please provide city location where the proceedings or conference was held for References 9, 15, 31, 38 and 39.	Provided for 9,15, 31 & 38. Replaced 39
Q5	AUTHOR: Please provide full conference title for Reference 31.	Provided full title
Q6	AUTHOR: Redundant issue number and publication date. Please update Reference 33.	Replaced reference
Q7	AUTHOR: Please expand journal title for Reference 34.	Gave full title
Q8	AUTHOR: Please provide page range for References 9 and 38–40.	Provide for 9 & 38, replaced 39. 40 is correct
Q9	AUTHOR: Please provide the name of the publisher and city location for Reference 41.	See replacement

WILEY-BLACKWELL

USING e-ANNOTATION TOOLS FOR ELECTRONIC PROOF CORRECTION

Required software to e-Annotate PDFs: Adobe Acrobat Professional or Adobe Reader (version 7.0 or above). (Note that this document uses screenshots from Adobe Reader X)
The latest version of Acrobat Reader can be downloaded for free at: http://get.adobe.com/uk/reader/

Once you have Acrobat Reader open on your computer, click on the Comment tab at the right of the toolbar:

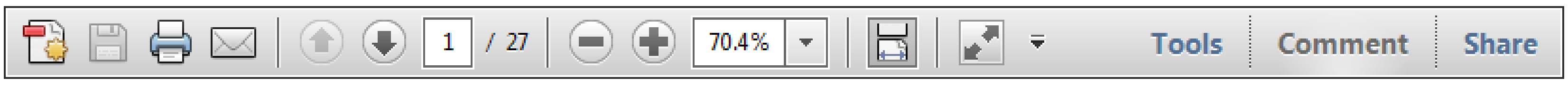

This will open up a panel down the right side of the document. The majority of tools you will use for annotating your proof will be in the Annotations section, pictured opposite. We've picked out some of these tools below:

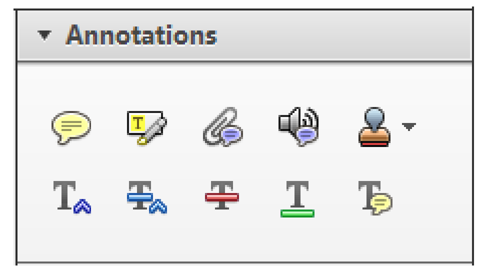

1. Replace (Ins) Tool – for replacing text.

Strikes a line through text and opens up a text box where replacement text can be entered.

How to use it

- Highlight a word or sentence.
- Click on the Replace (Ins) icon in the Annotations section.
- Type the replacement text into the blue box that appears.

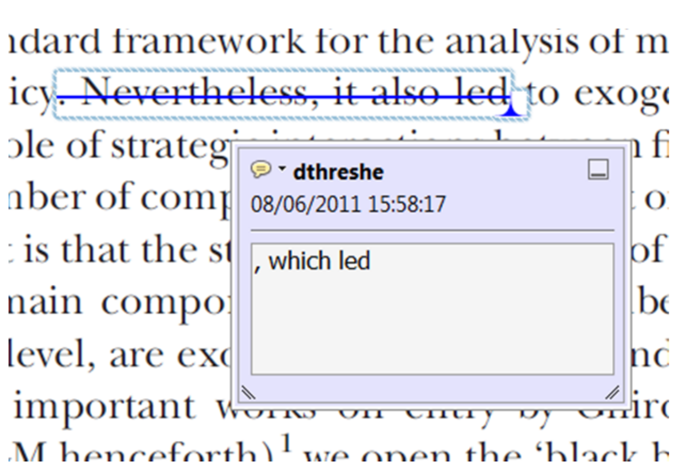

2. Strikethrough (Del) Tool – for deleting text.

Strikes a red line through text that is to be deleted.

How to use it

- Highlight a word or sentence.
- Click on the Strikethrough (Del) icon in the Annotations section.

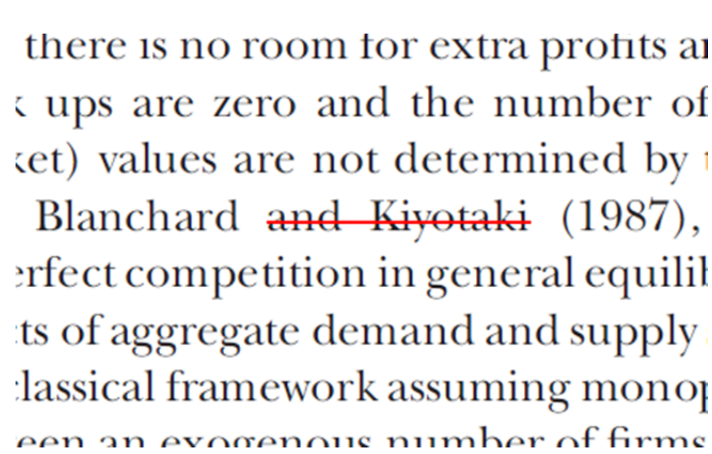

3. Add note to text Tool – for highlighting a section to be changed to bold or italic.

Highlights text in yellow and opens up a text box where comments can be entered.

How to use it

- Highlight the relevant section of text.
- Click on the Add note to text icon in the Annotations section.
- Type instruction on what should be changed regarding the text into the yellow box that appears.

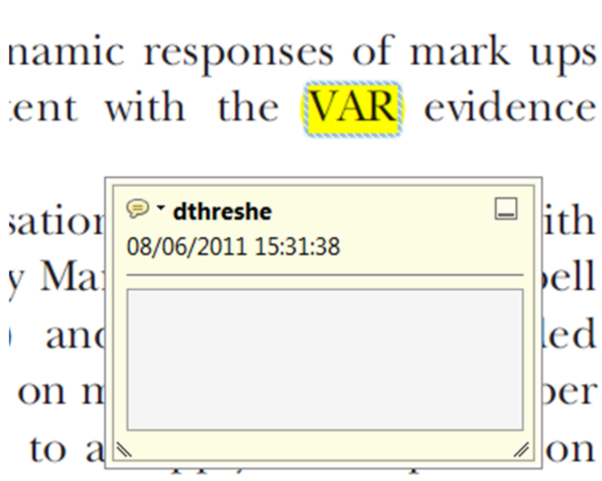

4. Add sticky note Tool – for making notes at specific points in the text.

Marks a point in the proof where a comment needs to be highlighted.

How to use it

- Click on the Add sticky note icon in the Annotations section.
- Click at the point in the proof where the comment should be inserted.
- Type the comment into the yellow box that appears.

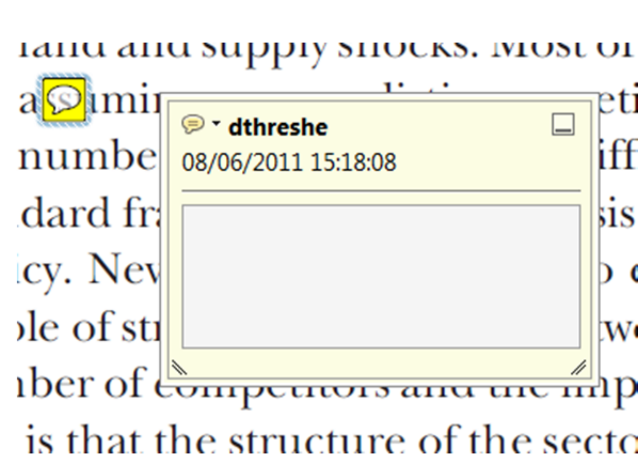

USING e-ANNOTATION TOOLS FOR ELECTRONIC PROOF CORRECTION

5. Attach File Tool – for inserting large amounts of text or replacement figures.

Inserts an icon linking to the attached file in the appropriate pace in the text.

How to use it

- Click on the Attach File icon in the Annotations section.
- Click on the proof to where you'd like the attached file to be linked.
- Select the file to be attached from your computer or network.
- Select the colour and type of icon that will appear in the proof. Click OK.

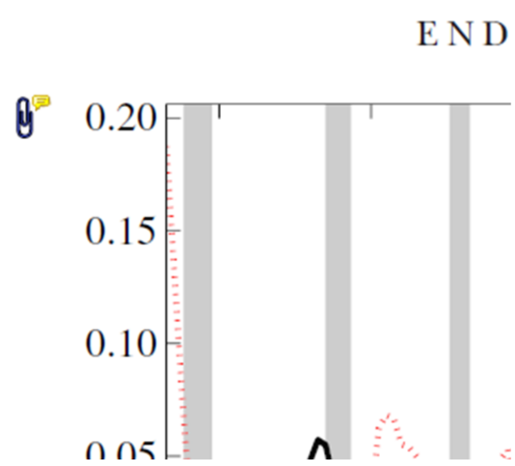

6. Add stamp Tool – for approving a proof if no corrections are required.

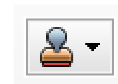

Inserts a selected stamp onto an appropriate place in the proof.

How to use it

- Click on the Add stamp icon in the Annotations section.
- Select the stamp you want to use. (The Approved stamp is usually available directly in the menu that appears).
- Click on the proof where you'd like the stamp to appear. (Where a proof is to be approved as it is, this would normally be on the first page).

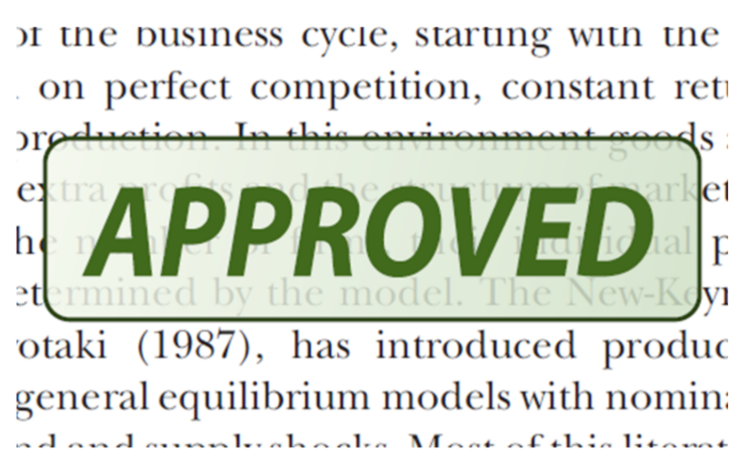

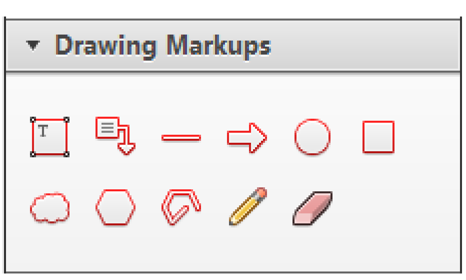

7. Drawing Markups Tools – for drawing shapes, lines and freeform annotations on proofs and commenting on these marks.

Allows shapes, lines and freeform annotations to be drawn on proofs and for comment to be made on these marks..

How to use it

- Click on one of the shapes in the Drawing Markups section.
- Click on the proof at the relevant point and draw the selected shape with the cursor.
- To add a comment to the drawn shape, move the cursor over the shape until an arrowhead appears.
- Double click on the shape and type any text in the red box that appears.

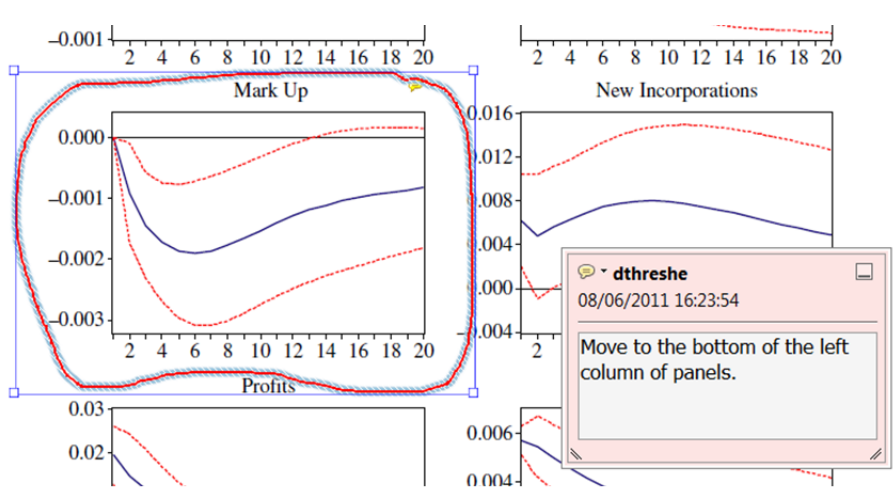

For further information on how to annotate proofs, click on the Help menu to reveal a list of further options:

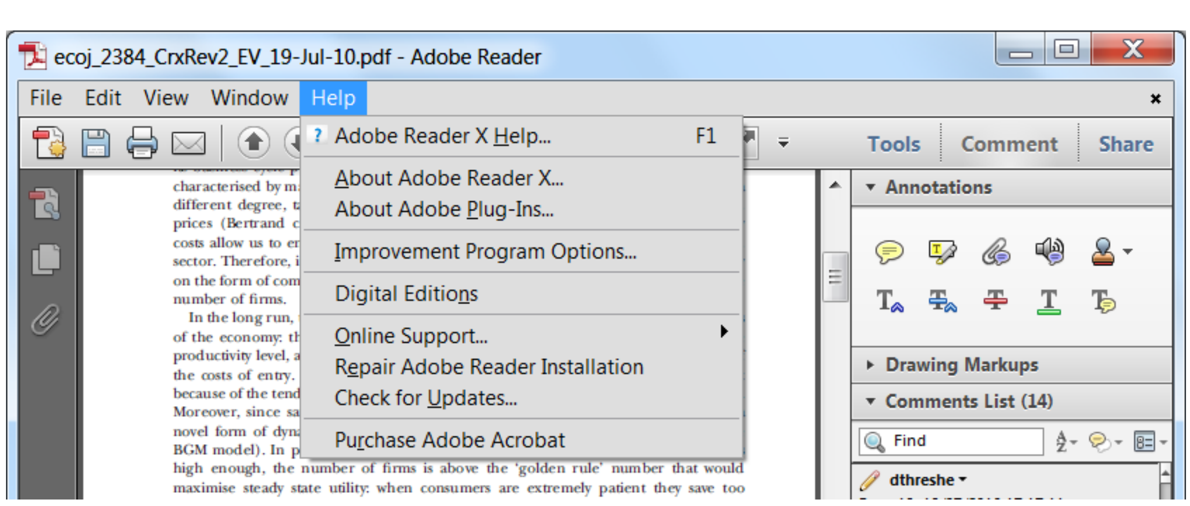

WILEY AUTHOR DISCOUNT CLUB

We would like to show our appreciation to you, a highly valued contributor to Wiley's publications, by offering a **unique 25% discount** off the published price of any of our books*.

All you need to do is apply for the **Wiley Author Discount Card** by completing the attached form and returning it to us at the following address:

The Database Group (Author Club)
John Wiley & Sons Ltd
The Atrium
Southern Gate
Chichester
PO19 8SQ
UK

Alternatively, you can **register online** at www.wileyeurope.com/go/authordiscount
Please pass on details of this offer to any co-authors or fellow contributors.

After registering you will receive your Wiley Author Discount Card with a special promotion code, which you will need to quote whenever you order books direct from us.

The quickest way to order your books from us is via our European website at:

http://www.wileyeurope.com

Key benefits to using the site and ordering online include:

- Real-time SECURE on-line ordering
- Easy catalogue browsing
- Dedicated Author resource centre
- Opportunity to sign up for subject-orientated e-mail alerts

Alternatively, you can order direct through Customer Services at:
cs-books@wiley.co.uk, or call +44 (0)1243 843294, fax +44 (0)1243 843303

So take advantage of this great offer and return your completed form today.

Yours sincerely,

V Leaver

Verity Leaver
Group Marketing Manager
author@wiley.co.uk

*TERMS AND CONDITIONS
This offer is exclusive to Wiley Authors, Editors, Contributors and Editorial Board Members in acquiring books for their personal use. There must be no resale through any channel. The offer is subject to stock availability and cannot be applied retrospectively. This entitlement cannot be used in conjunction with any other special offer. Wiley reserves the right to amend the terms of the offer at any time.

WILEY

REGISTRATION FORM
For Wiley Author Club Discount Card

To enjoy your 25% discount, tell us your areas of interest and you will receive relevant catalogues or leaflets from which to select your books. Please indicate your specific subject areas below.

Accounting [ ]
- Public [ ]
- Corporate [ ]

Chemistry [ ]
- Analytical [ ]
- Industrial/Safety [ ]
- Organic [ ]
- Inorganic [ ]
- Polymer [ ]
- Spectroscopy [ ]

Encyclopedia/Reference [ ]
- Business/Finance [ ]
- Life Sciences [ ]
- Medical Sciences [ ]
- Physical Sciences [ ]
- Technology [ ]

Earth & Environmental Science [ ]

Hospitality [ ]

Genetics [ ]
- Bioinformatics/ Computational Biology [ ]
- Proteomics [ ]
- Genomics [ ]
- Gene Mapping [ ]
- Clinical Genetics [ ]

Medical Science [ ]
- Cardiovascular [ ]
- Diabetes [ ]
- Endocrinology [ ]
- Imaging [ ]
- Obstetrics/Gynaecology [ ]
- Oncology [ ]
- Pharmacology [ ]
- Psychiatry [ ]

Non-Profit [ ]

Architecture [ ]

Business/Management [ ]

Computer Science [ ]
- Database/Data Warehouse [ ]
- Internet Business [ ]
- Networking [ ]
- Programming/Software Development [ ]
- Object Technology [ ]

Engineering [ ]
- Civil [ ]
- Communications Technology [ ]
- Electronic [ ]
- Environmental [ ]
- Industrial [ ]
- Mechanical [ ]

Finance/Investing [ ]
- Economics [ ]
- Institutional [ ]
- Personal Finance [ ]

Life Science [ ]

Landscape Architecture [ ]

Mathematics [ ]
Statistics [ ]

Manufacturing [ ]

Materials Science [ ]

Psychology [ ]
- Clinical [ ]
- Forensic [ ]
- Social & Personality [ ]
- Health & Sport [ ]
- Cognitive [ ]
- Organizational [ ]
- Developmental & Special Ed [ ]
- Child Welfare [ ]
- Self-Help [ ]

Physics/Physical Science [ ]

Please complete the next page /

I confirm that I am (*delete where not applicable):

a **Wiley** Book Author/Editor/Contributor* of the following book(s):
ISBN:
ISBN:

a **Wiley** Journal Editor/Contributor/Editorial Board Member* of the following journal(s):

SIGNATURE: ………………………………………………………………………………… Date: ……………………………………

PLEASE COMPLETE THE FOLLOWING DETAILS IN BLOCK CAPITALS:

TITLE: (e.g. Mr, Mrs, Dr) …………………… FULL NAME: ……………………………………………………………………………

JOB TITLE (or Occupation): ………

DEPARTMENT: ……

COMPANY/INSTITUTION: ……

ADDRESS: ……

……

TOWN/CITY: ………

COUNTY/STATE: ………

COUNTRY: ……

POSTCODE/ZIP CODE: ……

DAYTIME TEL: ……

FAX: ………

E-MAIL: ………

YOUR PERSONAL DATA
We, John Wiley & Sons Ltd, will use the information you have provided to fulfil your request. In addition, we would like to:

1. Use your information to keep you informed by post of titles and offers of interest to you and available from us or other Wiley Group companies worldwide, and may supply your details to members of the Wiley Group for this purpose.
   [ ] Please tick the box if you do **NOT** wish to receive this information

2. Share your information with other carefully selected companies so that they may contact you by post with details of titles and offers that may be of interest to you.
   [ ] Please tick the box if you do **NOT** wish to receive this information.

E-MAIL ALERTING SERVICE
We also offer an alerting service to our author base via e-mail, with regular special offers and competitions. If you **DO** wish to receive these, please opt in by ticking the box [ ].

If, at any time, you wish to stop receiving information, please contact the Database Group (databasegroup@wiley.co.uk) at John Wiley & Sons Ltd, The Atrium, Southern Gate, Chichester, PO19 8SQ, UK.

TERMS & CONDITIONS
This offer is exclusive to Wiley Authors, Editors, Contributors and Editorial Board Members in acquiring books for their personal use. There should be no resale through any channel. The offer is subject to stock availability and may not be applied retrospectively. This entitlement cannot be used in conjunction with any other special offer. Wiley reserves the right to vary the terms of the offer at any time.

PLEASE RETURN THIS FORM TO:
Database Group (Author Club), John Wiley & Sons Ltd, The Atrium, Southern Gate, Chichester, PO19 8SQ, UK author@wiley.co.uk
Fax: +44 (0)1243 770154